Bone marrow–on–a–chip replicates hematopoietic niche physiology *in vitro*

Yu-suke Torisawa[1,7], Catherine S Spina[1,2,7], Tadanori Mammoto[3], Akiko Mammoto[3], James C Weaver[1], Tracy Tat[3], James J Collins[1,2,4,5] & Donald E Ingber[1,3,6]

Current *in vitro* hematopoiesis models fail to demonstrate the cellular diversity and complex functions of living bone marrow; hence, most translational studies relevant to the hematologic system are conducted in live animals. Here we describe a method for fabricating 'bone marrow–on–a–chip' that permits culture of living marrow with a functional hematopoietic niche *in vitro* by first engineering new bone *in vivo*, removing it whole and perfusing it with culture medium in a microfluidic device. The engineered bone marrow (eBM) retains hematopoietic stem and progenitor cells in normal *in vivo*–like proportions for at least 1 week in culture. eBM models organ-level marrow toxicity responses and protective effects of radiation countermeasure drugs, whereas conventional bone marrow culture methods do not. This biomimetic microdevice offers a new approach for analysis of drug responses and toxicities in bone marrow as well as for study of hematopoiesis and hematologic diseases *in vitro*.

The bone marrow microenvironment contains a complex set of cellular, chemical, structural and physical cues necessary to maintain the viability and function of the hematopoietic system[1–5]. This hematopoietic niche regulates hematopoietic stem cells (HSCs), facilitating a delicate balance between self-renewal and differentiation into progenitor cells that produce all mature blood cell types[4,5]. Engineering an artificial bone marrow that reconstitutes natural marrow structure and function, and that can be maintained in culture, could be a powerful platform to study hematopoiesis and test new therapeutics. It has proven difficult, however, to recreate the complex bone marrow microenvironment needed to support the formation and maintenance of a complete, functional hematopoietic niche *in vitro*[6–9]. Although various *in vitro* culture systems have been developed to maintain and expand HSCs and progenitor cells[6–11], there is currently no method to recreate or study the intact bone marrow microenvironment *in vitro*. Therefore, studies on hematopoiesis commonly rely on animal models to ensure the presence of an intact bone marrow microenvironment that enables normal physiologic marrow responses[12–15]. Furthermore, although it has been reported that bone marrow can be engineered *in vivo*[16–19], no method exists to culture engineered bone marrow *in vitro*. To bridge the functional gap between *in vivo* and *in vitro* systems, we developed a method to produce a bone marrow–on–a–chip culture system that contains artificial bone and living marrow. The bone with marrow is first generated in mice and then explanted whole and maintained *in vitro* within a microfluidic device.

RESULTS

In vivo engineering of bone marrow

Tissue engineering methods have been used to induce the formation of new bone with a central marrow compartment *in vivo*[18–21]. To explore the possibility of engineering an artificial bone marrow that can be explanted whole, we microfabricated a poly(dimethylsiloxane) (PDMS) device with a central cylindrical cavity (1 mm high × 4 mm in diameter) with openings at both ends (**Fig. 1a**). We filled the hollow compartment with a type I collagen gel containing bone-inducing demineralized bone powder (DBP) and bone morphogenetic proteins (BMP2 and BMP4)[20–22] and implanted the device subcutaneously in the back of a mouse (**Supplementary Fig. 1**). Our goal was to engineer bone that would fill the cylindrical space within the implanted device so that it could be easily removed whole and inserted into a microfluidic system containing a similarly shaped chamber for *in vitro* culture (**Fig. 1a**,**b**). These initial studies resulted in the creation of new bone encasing a marrow compartment that formed within the PDMS device 4–8 weeks after subcutaneous implantation. Histological analysis revealed that the marrow was largely inhabited by adipocytes and that it exhibited a low level of hematopoietic cell contribution, even 8 weeks after implantation (**Fig. 1c**), as previously noted by others using similar tissue engineering approaches with bone-inducing materials[19–21].

The presence of large numbers of adipocytes in bone marrow can inhibit hematopoiesis[23]. To reduce adipocyte content

[1]Wyss Institute for Biologically Inspired Engineering, Harvard University, Boston, Massachusetts, USA. [2]Boston University School of Medicine, Boston, Massachusetts, USA. [3]Vascular Biology Program, Departments of Pathology and Surgery, Children's Hospital Boston and Harvard Medical School, Boston, Massachusetts, USA. [4]Howard Hughes Medical Institute, Boston University, Boston, Massachusetts, USA. [5]Department of Biomedical Engineering, Boston University, Boston, Massachusetts, USA. [6]School of Engineering and Applied Science, Harvard University, Cambridge, Massachusetts, USA. [7]These authors contributed equally to this work. Correspondence should be addressed to D.E.I. (don.ingber@wyss.harvard.edu).

RECEIVED 15 NOVEMBER 2013; ACCEPTED 4 APRIL 2014; PUBLISHED ONLINE 4 MAY 2014; DOI:10.1038/NMETH.2938

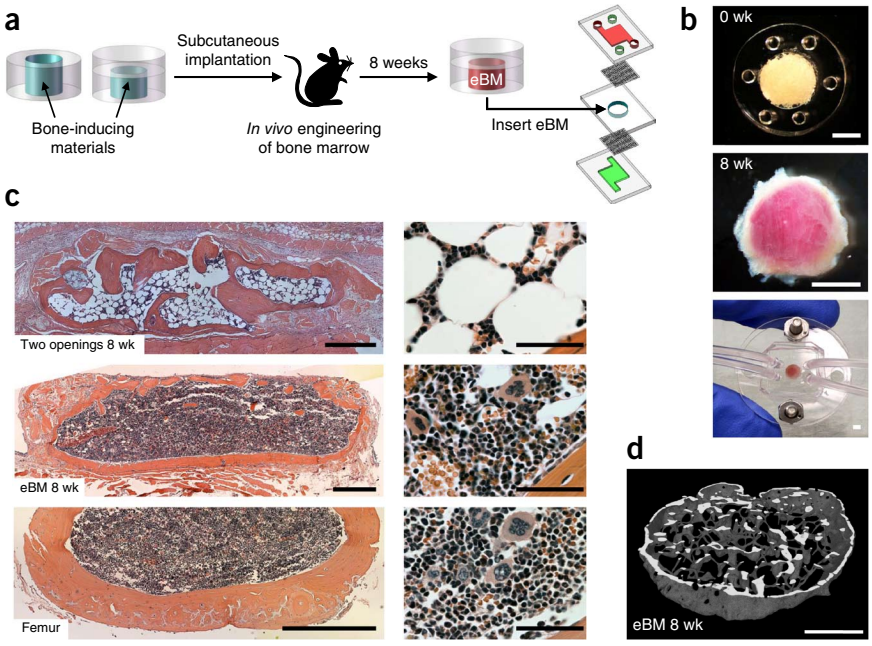

Figure 1 | *In vivo* bone marrow engineering. (**a**) Workflow to generate a bone marrow–on–a–chip system in which eBM is formed in a PDMS device *in vivo* and is then cultured in a microfluidic system. (**b**) Top, PDMS device containing bone-inducing materials in its central cylindrical chamber before implantation. Center, formed white cylindrical bone with pink marrow visible within eBM 8 weeks (wk) after implantation. Bottom, bone marrow chip microdevice used to culture the eBM *in vitro*. Scale bars, 2 mm. (**c**) Low- (left) and high-magnification views (right) of histological hematoxylin-and-eosin–stained sections of the eBM formed in the PDMS device with two openings (top) or one lower opening (center) at 8 weeks following implantation compared with a cross-section of bone marrow in a normal adult mouse femur (bottom). Scale bars, 500 and 50 μm for low and high magnification views, respectively. (**d**) Three-dimensional reconstruction of micro-computed tomography (micro-CT) data from eBM 8 weeks after implantation (average bone volume was 2.95 ± 0.25 mm^3; n = 3). Scale bar, 1 mm.

in the marrow, we sealed the top of the central cavity in the implanted device by adding a solid layer of PDMS to restrict access of cells or soluble factors from the overlying adipocyte-rich hypodermis to the bone-inducing materials while maintaining accessibility to the underlying muscle tissue through the lower opening (**Fig. 1a** and **Supplementary Fig. 1**). Subcutaneous implantation of this improved PDMS device resulted in the formation of a cylindrical disk of white, bone-like tissue containing a central region of blood-filled marrow over a period of 8 weeks (**Fig. 1b** and **Supplementary Fig. 2**). Histological analysis confirmed the presence of a shell of cortical bone of relatively uniform thickness surrounding marrow that was dominated by hematopoietic cells and that contained few adipocytes (**Fig. 1c**). Comparison of histological sections of the eBM to sections from an intact femur confirmed that the morphology of the eBM was nearly identical to that of natural bone marrow (**Fig. 1c**).

Micro-computed tomographic (micro-CT) analysis of the eBM demonstrated that the newly formed cortical shell of bone also contained an ordered internal trabecular network that closely resembles the intricate architecture found in normal adult mouse vertebrae (**Supplementary Fig. 3**) and that is known to be supportive of HSCs[24] (**Fig. 1d**). Compositional analysis using energy-dispersive X-ray spectroscopy (EDS) also showed that the calcium and phosphorous content of the eBM were indistinguishable from that of natural trabecular bone (**Supplementary Fig. 3**).

Characterization of engineered bone marrow

Interactions between CXCL12 expressed on the surfaces of various cell types in the bone marrow (such as osteoblasts[25], perivascular endothelial and perivascular stromal cells[26]) and its cognate receptor CXCR4 on the surfaces of HSCs and hematopoietic progenitor cells are critical for the recruitment, retention and maintenance of HSCs[26–28]. Immunohistochemical analysis confirmed that both of these key hematopoietic regulators were expressed in their normal positions in the eBM: CXCL12 localized to cells lining the inner surface of the bone and blood vessels, and CXCR4 was expressed by clusters of lymphoid cells in the endosteal and perivascular niches (**Fig. 2a–d**). We also confirmed that key hematopoietic niche cells[3] including perivascular nestin$^+$ cells and leptin receptor$^+$ cells, as well as CD31$^+$ vascular endothelial cells, resided in their normal positions (**Supplementary Fig. 4**).

To rigorously characterize the hematopoietic content of the engineered marrow, we harvested cells from the eBM immediately after surgical removal and analyzed them by flow cytometry. The cellular components of the marrow contained within the eBM were compared to hematopoietic populations isolated from femur bone marrow and peripheral blood from the same mice (**Fig. 2e**,**g**). Devices harvested 4 and 8 weeks after implantation contained all blood cell types, including HSCs that are not recognized by a mixture of Lin antibodies that recognize mature, lineage-restricted blood cells (Lin$^-$Sca1$^+$cKit$^+$CD34$^{+/-}$, Lin$^-$Sca1$^+$cKit$^+$CD150$^{+/-}$CD48$^{-/+}$) and hematopoietic progenitor cells identified by four different marker sets (Lin$^-$Sca1$^+$, Lin$^-$cKit$^+$, Lin$^-$CD34$^+$, Lin$^-$CD135$^+$), as well as mature erythrocytes (Ter119$^+$), lymphocytes (T cells, CD45$^+$CD3$^+$; B cells, CD45$^+$CD19$^+$) and myeloid cells (CD45$^+$Mac1$^{+/-}$Gr1$^{+/-}$). The eBM harvested 4 weeks after implantation did not appear to be fully developed, as indicated by a lower proportion of HSCs and hematopoietic progenitor cells compared to that in normal marrow (**Fig. 2f**,**h**). However, cells harvested from the eBM 8 weeks after implantation exhibited a completely normal distribution of HSCs, hematopoietic progenitors and differentiated blood cells from all lineages that was nearly identical to that displayed by natural bone marrow (**Fig. 2f**,**h** and **Supplementary Figs. 5** and **6**).

In summary, our modified strategy for eBM produced a cylindrical disk of cortical and trabecular bone (**Supplementary Fig. 3**) containing marrow with a hematopoietic cell composition nearly identical to that of natural bone marrow. The presence of key cellular and molecular components of the hematopoietic niche suggests that the cellular content of the eBM closely resembles the natural bone environment.

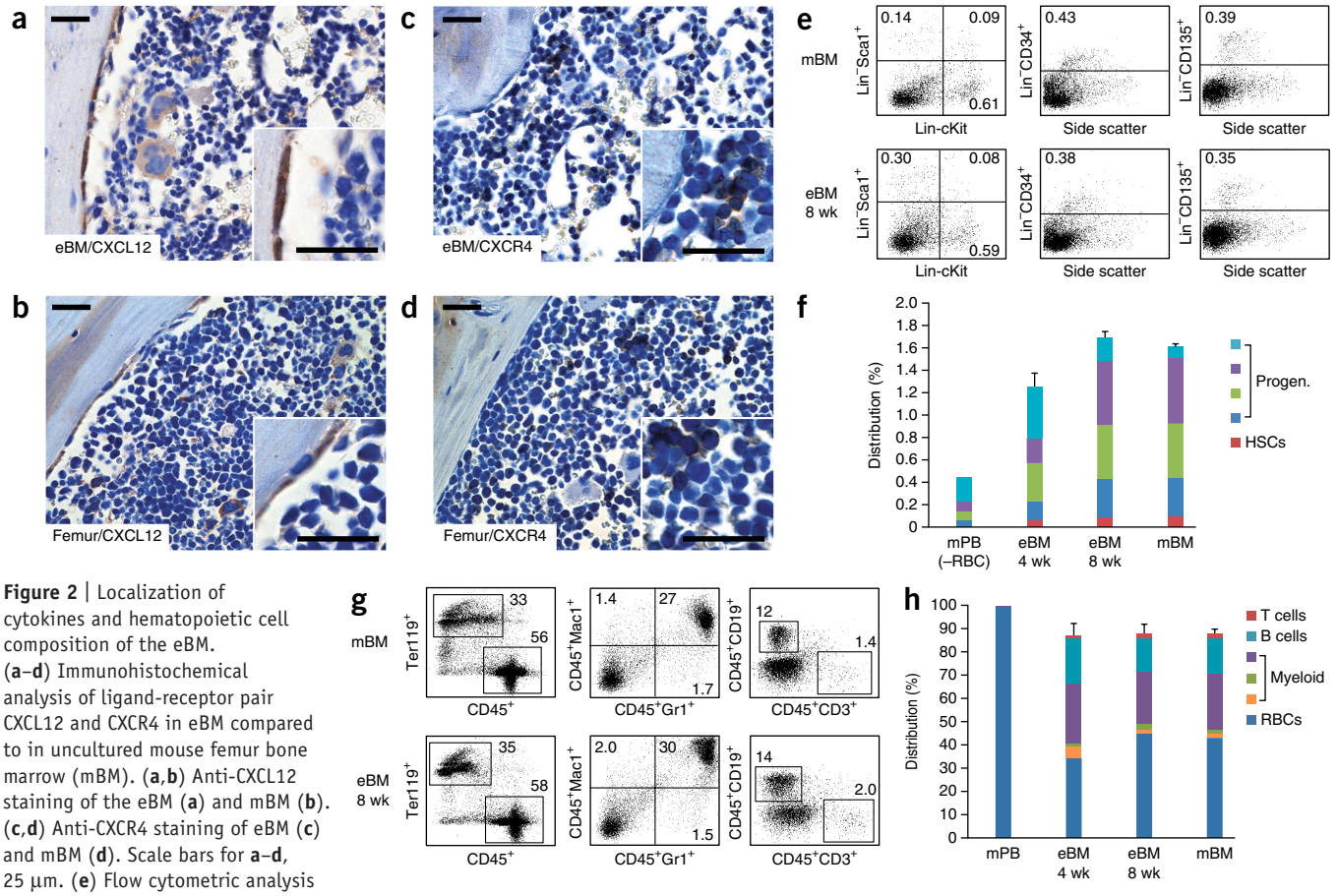

Figure 2 | Localization of cytokines and hematopoietic cell composition of the eBM. (**a**–**d**) Immunohistochemical analysis of ligand-receptor pair CXCL12 and CXCR4 in eBM compared to in uncultured mouse femur bone marrow (mBM). (**a**,**b**) Anti-CXCL12 staining of the eBM (**a**) and mBM (**b**). (**c**,**d**) Anti-CXCR4 staining of eBM (**c**) and mBM (**d**). Scale bars for **a**–**d**, 25 µm. (**e**) Flow cytometric analysis of HSCs and hematopoietic progenitor (progen.) cells within the Lin⁻ cell subpopulation isolated from mBM and eBM isolated 8 weeks (wk) after subcutaneous implantation. Numbers inside individual gates indicate the proportion of these cells as a percentage of the total cell population isolated from whole bone marrow. (**f**) Distribution of HSCs (Lin⁻Sca1⁺cKit⁺, red) and hematopoietic progenitor cells (Lin⁻Sca1⁺, cyan; Lin⁻cKit⁺, purple; Lin⁻CD34⁺, green; Lin⁻CD135⁺, blue) as quantified by flow cytometric analysis of mBM ($n = 6$), eBM at 4 ($n = 5$) or 8 weeks ($n = 5$) after implantation, or mouse peripheral blood (mPB) ($n = 1$) that underwent erythrocyte lysis to facilitate detection of rare HSCs. (**g**,**h**) Flow cytometry plots (**g**) and distribution (**h**) of matured, lineage-restricted cell types including erythrocytes (Ter119⁺, blue), myeloid cells (CD45⁺Mac1⁺, orange; CD45⁺Gr1⁺, green; CD45⁺Mac1⁺Gr1⁺, purple), B cells (CD45⁺CD19⁺, cyan) and T cells (CD45⁺CD3⁺, red) in mBM ($n = 6$), eBM at 4 weeks ($n = 5$), eBM at 8 weeks ($n = 5$) and intact mPB ($n = 1$). Error bars, s.e.m.

In vitro culture of engineered bone marrow

To determine whether the eBM could maintain a functional hematopoietic system *in vitro*, we surgically removed the eBM formed 8 weeks after implantation from the mouse, punctured it in multiple places with a surgical needle to permit fluid access and cultured it in another clear PDMS microfluidic device containing a similarly shaped cylindrical central chamber that is separated from overlying and underlying microfluidic channels by porous membranes (**Fig. 1a**,**b**). To maintain the cellular viability of the eBM, we perfused culture medium through the top and bottom channels using a syringe pump at an optimal rate (1 µl/min) (**Supplementary Fig. 7**) once the eBM was inserted into the central chamber and the surrounding porous membranes and microchannel layers were attached. The eBM was cultured *in vitro* for 4 or 7 d within the bone marrow–chip microsystem (**Fig. 1b**), which covers a time period that is commonly used to test for drug efficacies and toxicities *in vitro*[29,30]. The cultured bone and marrow retained their morphology during this time, including the distribution of CXCL12-expressing stromal cells (**Supplementary Fig. 8**). Stroma-supported culture systems represent the current benchmark for maintaining survival of HSCs and hematopoietic progenitor cells *in vitro*[7,31]. Thus, we used flow cytometric analysis to compare the hematopoietic cellular composition of the cultured bone marrow–on–a–chip to that of marrow isolated from mouse femur cultured for the same amount of time on a stromal 'feeder' cell layer (**Supplementary Fig. 9**). Because past work has shown that the addition of cytokines is required to maintain or expand HSCs and their progenitors[6,7], and because serum can suppress the marrow-reconstituting activity of HSCs[32], the stroma-supported cultures were maintained in serum-free medium supplemented with cytokines (mSCF, mIL-11, mFLt-3 ligand and hLDL) that have been shown by others to more efficiently maintain and expand both HSCs and hematopoietic progenitor cell populations *in vitro*[33]. Our analysis revealed that there was no significant difference in cell viability after 4 or 7 d of culture in the microfluidic eBM device compared to the static stroma-supported culture (**Supplementary Fig. 10**). However, bone marrow cultured on stroma exhibited a significant decrease ($P < 0.0005$) in the number of long-term HSCs (Lin⁻CD150⁺ CD48⁻ cells) and a concomitant increase ($P < 0.0005$) in hematopoietic progenitor cells (Lin⁻CD34⁺, Lin⁻Sca1⁺, Lin⁻cKit⁺) relative to cells freshly isolated from natural mouse bone marrow (**Fig. 3a**,**b**). Thus, the long-term HSCs, which are the only cells capable of long-term

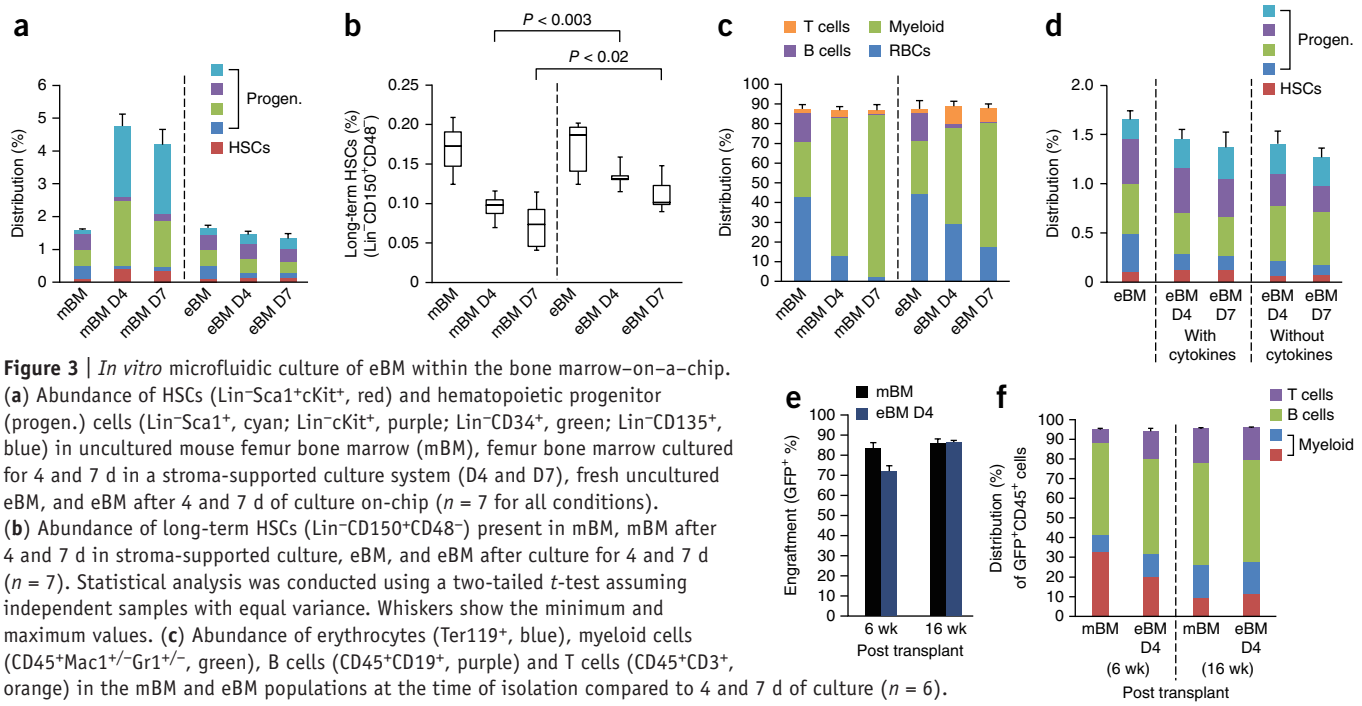

Figure 3 | *In vitro* microfluidic culture of eBM within the bone marrow–on–a–chip. (**a**) Abundance of HSCs (Lin⁻Sca1⁺cKit⁺, red) and hematopoietic progenitor (progen.) cells (Lin⁻Sca1⁺, cyan; Lin⁻cKit⁺, purple; Lin⁻CD34⁺, green; Lin⁻CD135⁺, blue) in uncultured mouse femur bone marrow (mBM), femur bone marrow cultured for 4 and 7 d in a stroma-supported culture system (D4 and D7), fresh uncultured eBM, and eBM after 4 and 7 d of culture on-chip ($n = 7$ for all conditions). (**b**) Abundance of long-term HSCs (Lin⁻CD150⁺CD48⁻) present in mBM, mBM after 4 and 7 d in stroma-supported culture, eBM, and eBM after culture for 4 and 7 d ($n = 7$). Statistical analysis was conducted using a two-tailed *t*-test assuming independent samples with equal variance. Whiskers show the minimum and maximum values. (**c**) Abundance of erythrocytes (Ter119⁺, blue), myeloid cells (CD45⁺Mac1$^{+/-}$Gr1$^{+/-}$, green), B cells (CD45⁺CD19⁺, purple) and T cells (CD45⁺CD3⁺, orange) in the mBM and eBM populations at the time of isolation compared to 4 and 7 d of culture ($n = 6$). (**d**) Abundance of HSCs and hematopoietic progenitor cells from fresh, uncultured eBM compared to 4 and 7 d of culture with and without supplemental cytokines (SCF, IL-11, Flt-3, LDL) ($n = 6$). (**e**) Extent of bone marrow engraftment in lethally irradiated mice transplanted with 2.5 × 10^5 GFP⁺ cells from uncultured mBM or isolated from the eBM following 4 d of *in vitro* culture on-chip. Engraftment is presented as percentage of GFP⁺ cells in the lymphoid population (CD45⁺) of peripheral blood measured 6 and 16 weeks (wk) after transplantation to confirm retention of functional hematopoietic progenitor cells and HSCs, respectively ($n = 3$). (**f**) Distribution of differentiated blood cells within the engrafted CD45⁺ population from mBM and eBM D4 transplants at 6 and 16 weeks after intravenous injection into lethally irradiated mice. Differentiated cell types include T cells (CD45⁺CD3⁺, purple), B cells (CD45⁺CD19⁺, green) and myeloid cells (CD45⁺Mac1⁺, blue; CD45⁺Gr1⁺, red) ($n = 3$). Error bars, s.e.m.

self-renewal and multilineage potential, appeared to be differentiating into more specialized progenitor cells in the static stroma-supported culture system, as previously reported[6–9]. In contrast, the number and distribution of HSCs and hematopoietic progenitor cells in the eBM cultured for up to 7 d on-chip were maintained in similar proportions to those of freshly harvested bone marrow (**Fig. 3a**). The bone marrow–on–a–chip enabled maintenance of a significantly higher proportion of long-term HSCs while more effectively maintaining the distribution of mature blood cells compared to the stroma-supported cultures (**Fig. 3b**,**c**). Interestingly, although the proportions of hematopoietic cells were retained over this culture period, there was no significant difference in the number or viability of cells cultured on-chip for 7 d compared to 4 d; hence, the HSCs and hematopoietic progenitor cells appeared to remain relatively quiescent in the marrow-on-a-chip microdevice. Moreover, although addition of exogenous (and expensive) cytokines, including mSCF, mIL-11, mFLt-3 ligand and hLDL, are critical for maintenance of these cell populations in conventional stroma-supported cultures[6,7,33], their removal from culture medium had little effect on the distribution of HSCs and hematopoietic progenitors in the cultured eBM (**Fig. 3d**). Thus, the eBM contained a functional hematopoietic niche that behaved in an autonomous fashion to support the continued survival of these critical blood-forming stem and progenitor cells *in vitro*. Blood cell populations could be maintained in normal proportions for at least 1 week under microfluidic flow *in vitro*, even in the absence of exogenous cytokines.

To confirm that the HSCs and hematopoietic progenitor cells retained in the cultured bone marrow–on–a–chip remained truly functional, we evaluated their self-renewal and differentiation capabilities by testing engraftment and hematopoietic reconstitution potential following transplantation into lethally irradiated, syngeneic recipient mice. Cells within the marrow compartments of eBMs that were formed in GFP-expressing animals and cultured on-chip for 4 d were harvested and transplanted into γ-irradiated mice; results were compared to those from irradiated mice transplanted with cells from freshly harvested bone marrow from mouse femur. Total engraftment was assessed in the peripheral blood of recipient mice 6 and 16 weeks after transplantation to confirm the presence of functional short- and long-term HSCs, respectively. Cells harvested from the eBM after 4 d in culture on-chip successfully engrafted the mice at a similar rate to that of freshly isolated, uncultured bone marrow (**Fig. 3e**) and repopulated all differentiated blood cell lineages (**Fig. 3f**), showing 70% and 85% engraftment by 6 and 16 weeks after transplantation, respectively. These data confirmed that the hematopoietic compartment of the eBM retained fully functional, self-renewing, multipotent HSCs after it was cultured in the microfluidic bone marrow chip for 4 d *in vitro*.

In vitro model for radiation toxicity

The functionality and organ-level responsiveness of the bone marrow–on–a–chip were tested by exposing the eBM to varying doses of γ-radiation to determine whether this method could be used as an *in vitro* model for radiation toxicity, which currently can only be studied in live animals. Live mice, eBMs cultured on-chip and marrow cells maintained in stroma-supported culture were exposed to 1- and 4-Gy doses of γ-radiation,

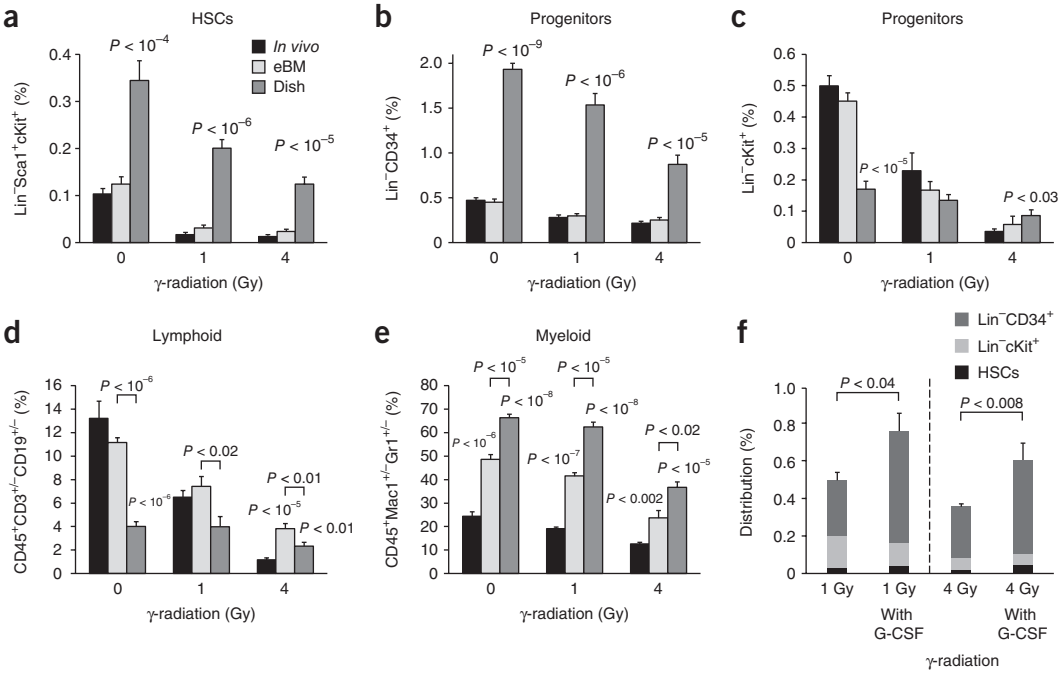

Figure 4 | Radiation toxicity of the bone marrow–on–a–chip. (**a**–**e**) Effects of γ-radiation on the abundance of HSCs (**a**), hematopoietic progenitors (**b**,**c**), lymphoid cells (**d**) and myeloid cells (**e**) within bone marrow freshly isolated from femurs of living mice (*in vivo*), eBM cultured on-chip for 4 d (eBM) or 4-d-old stroma-supported cultures (Dish) ($n = 5$). (**f**) Effect of G-CSF on the abundance of HSCs ($Lin^-Sca1^+cKit^+$ cells, black) and hematopoietic progenitor cells (Lin^-cKit^+, light gray; Lin^-CD34^+, dark gray) in eBM cultured on-chip for 4 d ($n = 5$). Statistical analysis was conducted using a two-tailed *t*-test assuming independent samples with equal variance. Error bars, s.e.m.; *P* values above individual bars represent comparisons between *in vivo* and experimental samples; brackets represent comparisons between experimental samples.

which have been shown to produce marrow toxicity in mice[34], and were maintained in culture. In measurements made 4 d after radiation exposure, we detected a statistically significant, radiation dose–dependent decrease in the proportion of HSCs, hematopoietic progenitors, lymphoid cells and myeloid cells (**Fig. 4a**–**e**), which closely mimics what is observed in the bone marrow of live irradiated mice. Interestingly, the proportion of HSCs ($Lin^-Sca1^+cKit^+$) or progenitors (Lin^-CD34^+) observed in eBM after exposure to 1- and 4-Gy doses of γ-radiation were nearly identical to the proportions measured in whole marrow from live mice that underwent similar irradiation. In contrast, the proportion of HSCs and progenitors were significantly lower ($P < 0.05$) in the stroma-supported culture after 4-Gy irradiation compared to after 1-Gy irradiation. Various types of marrow cells (HSCs, progenitors, lymphoid cells and myeloid cells) cultured on stroma also exhibited suppressed responses, and all were significantly more resistant ($P < 0.05$) to the effects of radiation toxicity (**Fig. 4a**–**e** and **Supplementary Fig. 11**).

To further evaluate the functional relevance and power of our system, we tested the effects of administering granulocyte colony–stimulating factor (G-CSF), which has been shown to accelerate recovery and prevent potentially lethal bone marrow failure following radiation exposure *in vivo*[35]. When G-CSF was added to the eBM cultured on-chip 1 d after exposure to γ-radiation, samples analyzed 3 d later demonstrated a significant increase in the total number of HSCs ($Lin^-Sca1^+cKit^+$) and hematopoietic progenitor cells (Lin^-cKit^+, Lin^-CD34^+) compared to untreated bone marrow chips that were similarly irradiated (**Fig. 4f**). These findings suggest that G-CSF induced proliferation of HSCs and hematopoietic progenitor cells in the bone marrow chip *in vitro*, as previously reported *in vivo*[35]. These data clearly demonstrate that the bone marrow–on–a–chip faithfully mimicked the natural physiological response of living bone marrow to clinically relevant doses of γ-radiation and to a validated radiation countermeasure drug (G-CSF), whereas conventional stroma-supported cultures do not.

DISCUSSION

Our bone marrow–on–a–chip fabrication strategy provides a proof of concept for the creation of an organ-on-chip device that reconstitutes and sustains an intact, functional, living bone marrow when cultured *in vitro*. This strategy differs substantially from conventional tissue engineering approaches in which materials or living cells are implanted *in vivo* without geometric constraint and without any intent of removing the newly formed organ and maintaining its viability *ex vivo*. Although we regenerated the complex structural, physical and cellular microenvironment of whole bone marrow by employing *in vivo* tissue engineering techniques, we then leveraged microfluidic strategies to deliver nutrients, chemicals and other soluble signals in a fashion that supports the continued viability and function of this engineered organ *in vitro*. This also differs from most organ-on-chip methods that use microengineering and microfluidics approaches to model tissue architecture, cell-cell relationships, chemical gradients and the mechanical microenvironment and then populate the devices with cultured cell lines or isolated stem cells[36].

Our *in vivo* engineering approach enabled us to reconstitute hematopoietic niche physiology and restore complex tissue-level functions of natural bone marrow. The eBM autonomously

produces the factors necessary to support the maintenance and function of the hematopoietic system *in vitro*, which offers a major practical advantage over existing culture systems in that expensive growth supplements can be removed from the culture medium or greatly reduced. Another advantage is that the bone marrow–on–a–chip supports HSCs and progenitor cells in normal *in vivo*–like proportions relative to the other hematopoietic cell populations and maintains their spatial positions within a fully formed three-dimensional bone marrow niche *in vitro*. These features of the bone marrow–on–a–chip are likely key to its ability to preserve complex functionalities of the whole organ that cannot be replicated by conventional stroma-supported cultures. Notably, the use of microfluidics also enables analysis of responses under flow, which is important for both the regulation of marrow physiology[5,6,10,37,38] and the study of pharmacokinetic and pharmacodynamic behaviors of drugs that are critical for evaluation of their clinical behavior.

The eBM cultured on-chip mimics complex tissue-level responses to radiation toxicity normally observed only *in vivo* and to a therapeutic countermeasure agent (G-CSF) that is known to accelerate recovery from radiation-induced toxicity in patients[39]. Thus, this biomimetic microsystem could serve as a valuable *in vitro* replacement for whole animals in the testing and development of drugs and other medical countermeasures that might protect against radiation poisoning in the future. The completeness of our organ mimic permits us to recapitulate the physiologic responses of the whole hematopoietic niche to clinically relevant cues (such as cytokines, drugs and radiation), whereas conventional cell cultures do not. This finding underscores the novelty of maintaining functional marrow containing multiple components of the hematopoietic niche *in vitro* rather than merely culturing particular hematopoietic cell types.

The bone marrow–on–a–chip provides an interesting alternative to animal models because it offers the ability to manipulate individual hematopoietic cell populations (such as genetically or using drugs), or to insert other cell types (such as tumor cells) *in vitro*, before analyzing the response of the intact marrow to relevant clinical challenges, including radiation or pharmaceuticals. It also might be possible to generate human bone marrow models: for example, an eBM could be engineered in immunocompromised mice (such as NOD.Cg-*Prkdc*^{scid}*Il2rg*^{tm1Wjl}/Sz; NSG) that have their endogenous marrow cells replaced with human hematopoietic cells.

The ability to produce trabecular bone with architectural and compositional properties similar to those of natural bone offers a way to produce bones of predefined size and shape, and it could represent a new method for the study of bone biology, remodeling and pathophysiology *in vitro*. Therefore, the bone marrow–on–a–chip is a powerful method to accelerate discovery and development in a wide range of biomedical fields ranging from hematology, oncology and drug discovery to tissue engineering.

METHODS

Methods and any associated references are available in the online version of the paper.

Note: Any Supplementary Information and Source Data files are available in the online version of the paper.

ACKNOWLEDGMENTS

We thank G.Q. Daley for guidance and helpful discussions and P.L. Wenzel, N. Arora, E. Jiang, A. Jiang, B. Mosadegh, D. Huh, A. Bahinski and G.A. Hamilton for their technical assistance and advice. This work was supported by the Wyss Institute for Biologically Inspired Engineering at Harvard University, the Defense Advanced Research Projects Agency under Cooperative Agreement Number W911NF-12-2-0036, and the US Food and Drug Administration (FDA) HHSF223201310079C.

AUTHOR CONTRIBUTIONS

Y.-s.T., C.S.S. and D.E.I. conceived of the experiments; Y.-s.T. and C.S.S. performed the experiments, designed research and analyzed data with assistance from T.M., A.M., J.C.W., T.T., J.J.C. and D.E.I. Y.-s.T., C.S.S. and D.E.I. wrote the manuscript.

COMPETING FINANCIAL INTERESTS

The authors declare no competing financial interests.

1. Sacchetti, B. *et al.* Self-renewing osteoprogenitors in bone marrow sinusoids can organize a hematopoietic microenvironment. *Cell* **131**, 324–336 (2007).
2. Chan, C.K.F. *et al.* Endochondral ossification is required for haematopoietic stem-cell niche formation. *Nature* **457**, 490–494 (2009).
3. Méndez-Ferrer, S. Mesenchymal and haematopoietic stem cells form a unique bone marrow niche. *Nature* **466**, 829–834 (2010).
4. Orkin, S.H. & Zon, L.I. Hematopoiesis: an evolving paradigm for stem cell biology. *Cell* **132**, 631–644 (2008).
5. Wang, L.D. & Wagers, A.J. Dynamic niches in the origination and differentiation of haematopoietic stem cells. *Nat. Rev. Mol. Cell Biol.* **12**, 643–655 (2011).
6. Di Maggio, N. *et al.* Toward modeling the bone marrow niche using scaffold-based 3D culture systems. *Biomaterials* **32**, 321–329 (2011).
7. Takagi, M. Cell processing engineering for *ex-vivo* expansion of hematopoietic cells. *J. Biosci. Bioeng.* **99**, 189–196 (2005).
8. Nichols, J.E. *et al.* *In vitro* analog of human bone marrow from 3D scaffolds with biomimetic inverted colloidal crystal geometry. *Biomaterials* **30**, 1071–1079 (2009).
9. Cook, M.M. *et al.* Micromarrows-three-dimensional coculture of hematopoietic stem cells and mesenchymal stromal cells. *Tissue Eng. Part C Methods* **18**, 319–328 (2012).
10. Csaszar, E. *et al.* Rapid expansion of human hematopoietic stem cells by automated control of inhibitory feedback signaling. *Cell Stem Cell* **10**, 218–229 (2012).
11. Boitano, A.E. *et al.* Aryl hydrocarbon receptor antagonists promote the expansion of human hematopoietic stem cells. *Science* **329**, 1345–1348 (2010).
12. Cao, X. *et al.* Irradiation induces bone injury by damaging bone marrow microenvironment for stem cells. *Proc. Natl. Acad. Sci. USA* **108**, 1609–1614 (2011).
13. Askmyr, M., Quach, J. & Purton, L.E. Effects of the bone marrow microenvironment on hematopoietic malignancy. *Bone* **48**, 115–120 (2011).
14. Greenberger, J.S. & Epperly, M. Bone marrow-derived stem cells and radiation response. *Semin. Radiat. Oncol.* **19**, 133–139 (2009).
15. Meads, M.B., Hazlehurst, L.A. & Dalton, W.S. The bone marrow microenvironment as a tumor sanctuary and contributor to drug resistance. *Clin. Cancer Res.* **14**, 2519–2526 (2008).
16. Scotti, C. *et al.* Engineering of a functional bone organ through endochondral ossification. *Proc. Natl. Acad. Sci. USA* **110**, 3997–4002 (2013).
17. Lee, J. *et al.* Implantable microenvironments to attract hematopoietic stem/cancer cells. *Proc. Natl. Acad. Sci. USA* **109**, 19638–19643 (2012).
18. Reddi, A.H. & Huggins, C. Biochemical sequences in the transformation of normal fibroblasts in adolescent rats. *Proc. Natl. Acad. Sci. USA* **69**, 1601–1605 (1972).
19. Krupnick, A.S., Shaaban, S., Radu, A. & Flake, A.W. Bone marrow tissue engineering. *Tissue Eng.* **8**, 145–155 (2002).
20. Chen, B. *et al.* Homogeneous osteogenesis and bone regeneration by demineralized bone matrix loading with collagen-targeting bone morphogenetic protein-2. *Biomaterials* **28**, 1027–1035 (2007).

21. Schwartz, Z. *et al.* Differential effects of bone graft substitutes on regeneration of bone marrow. *Clin. Oral Implants Res.* **19**, 1233–1245 (2008).
22. Ekelund, A., Brosjö, O. & Nilsson, O.S. Experimental induction of heterotopic bone. *Clin. Orthop. Relat. Res.* **263**, 102–112 (1991).
23. Naveiras, O. *et al.* Bone-marrow adipocytes as negative regulators of the haematopoietic microenvironment. *Nature* **460**, 259–263 (2009).
24. Xie, Y. *et al.* Detection of functional haematopoetic stem cell niche using real-time imaging. *Nature* **457**, 97–101 (2009).
25. Calvi, L.M. *et al.* Osteoblastic cells regulate the haematopoietic stem cell niche. *Nature* **425**, 841–846 (2003).
26. Ding, L. & Morrison, S.J. Haematopoietic stem cells and early lymphoid progenitors occupy distinct bone marrow niches. *Nature* **495**, 231–235 (2013).
27. Zou, Y.-R. *et al.* Function of the chemokine receptor CXCR4 in haematopoiesis and in cerebellar development. *Nature* **393**, 595–599 (1998).
28. Peled, A. *et al.* The chemokine SDF-1 stimulates integrin-mediated arrest of $CS34^+$ cells on vascular endothelium under shear flow. *J. Clin. Invest.* **104**, 1199–1211 (1999).
29. Olaharski, A.J. *et al. In vitro* to *in vivo* concordance of a high throughput assay of bone marrow toxicity across a diverse set of drug candidates. *Toxicol. Lett.* **188**, 98–103 (2009).
30. Hoeksema, K.A. *et al.* Systematic *in-vitro* evaluation of the NCI/NIH Developmental Therapeutics Program Approved Oncology Drug Set for the identification of a candidate drug repertoire for *MLL*-rearranged leukemia. *OncoTargets and Therapy* **4**, 149–168 (2011).
31. Dexter, T.M., Wright, E.G., Krizsa, F. & Lajtha, L.G. Regulation of haemopoietic stem cells proliferation in long term bone marrow cultures. *Biomedicine* **27**, 344–349 (1977).
32. Bryder, D. & Jacobsen, E.W. Interleukin-3 supports expansion of long-term multilineage repopulating activity after multiple stem cell divisions *in vitro*. *Blood* **96**, 1748–1755 (2000).
33. Miller, C.L. & Eaves, C.J. Expansion *in vitro* of adult murine hematopoietic stem cells with transplantable lympho-myeloid reconstituting ability. *Proc. Natl. Acad. Sci. USA* **94**, 13648–13653 (1997).
34. Williams, J.P. *et al.* Animal models for medical countermeasures to radiation exposure. *Radiat. Res.* **173**, 557–578 (2010).
35. Cary, L.H., Ngudiankama, B.F., Salber, R.E., Ledney, G.D. & Whitnall, M.H. Efficacy of radiation countermeasures depends on radiation quality. *Radiat. Res.* **177**, 663–675 (2012).
36. Huh, D. *et al.* Microengineered physiological biomimicry: organs-in-chips. *Lab Chip* **12**, 2156–2164 (2012).
37. Schwartz, R.M., Palsson, B.O. & Emerson, S.G. Rapid medium perfusion rate significantly increase the productivity and longevity of human bone marrow cultures. *Proc. Natl. Acad. Sci. USA* **88**, 6760–6764 (1991).
38. Wendt, D., Stroebel, S., Jakob, M., John, G.T. & Martin, I. Uniform tissues engineered by seeding and culturing cells in 3D scaffolds under perfusion at defined oxygen tensions. *Biorheology* **43**, 481–488 (2006).
39. Hérodin, F. & Drouet, M. Cytokine-based treatment of accidentally irradiated victims and new approaches. *Exp. Hematol.* **33**, 1071–1080 (2005).

ONLINE METHODS

Animals. CD-1 mice were purchased from Charles River Laboratories and C57BL/6 mice and C57BL/6-Tg(UBC-GFP)30Scha/J mice were from Jackson Laboratories. All animal studies were reviewed and approved by the Animal Care and Use Committee of Children's Hospital Boston. For both implantation of devices and transplant experiments, no randomization or blinding was completed. All transplanted mice and those implanted with devices were equivalent (age, sex, strain).

Bone-inducing materials. Demineralized bone powder (DBP) was prepared from femurs harvested from CD-1 mice[18]. The femurs were washed in sterile water, extracted with absolute ethanol and dehydrated with ether. The bones were crushed with a mortar and pestle and demineralized in 0.5 N HCl (50 mL/g) for 3 h at room temperature. After demineralization, DBP was washed with sterile water, extracted with absolute ethanol, dehydrated with ether and passed through a sieve with 250-μm pores. 3 mg DBP mixed with 30 μL solution of type I collagen gel (3 mg/mL, Cellmatrix Type I-A, Nitta Gelatin), 100 ng BMP2 (Alpha Diagnostic Intl.) and 100 ng BMP4 (Alpha Diagnostic Intl.) was placed in the central cylindrical cavity (1 mm high × 4 mm in diameter) of a device (1 mm high × 8 mm in diameter) (**Fig. 1a**,**b**), which was fabricated from poly(dimethylsiloxane) (PDMS) formed from prepolymer (Sylgard 184, Dow Corning) at a ratio of 10:1 base to curing agent and using biopsy punches (Miltex). To seal the top of the central cylindrical cavity, we bonded together a solid layer of PDMS (0.5 mm thick) and the device using a plasma etcher (SPI Plasma-Perp II, Structure Probe) in air for 30 s.

Implantation of bone-inducing materials. The PDMS devices filled with the bone-inducing materials were implanted subcutaneously on the backs of 8- to 12-week-old CD-1 mice or C57BL/6-Tg(UBC-GFP)30Scha/J mice and harvested 4 or 8 weeks after implantation (**Supplementary Fig. 1**). Because implantation of devices was completed in all animals procured or bred, a randomization procedure was not performed. The PDMS device with two openings permitted access between the bone-inducing materials and both the underlying muscle and overlying skin (**Fig. 1a** and **Supplementary Fig. 1**). The PDMS device with a single lower opening permitted access to only the muscle.

Histology and immunohistochemistry. Engineered bone marrow (eBM) harvested from mice 8 weeks after implantation, and femurs from the same mice, were collected and fixed in 4% paraformaldehyde at 4 °C for 24 h. Tissues were transferred into 70% ethanol and stored at room temperature until processed. Tissues were embedded in paraffin and sectioned for subsequent hematoxylin and eosin (H&E) staining, immunohistochemistry using anti-CXCL12 (SDF-1 beta; eBioscience, #14-7991-83) or anti-CXCR4 (UMB2; Novus Biologicals, #NBP1-95362) polyclonal antibodies, followed by anti-rabbit IgG conjugated to HRP (Vector Laboratories). Slides were counterstained with hematoxylin. Tissues were also embedded in Tissue-Tek O.C.T. (Sakura Finetek) and sectioned for subsequent immunofluorescence analysis using anti-CD31 (Abcom, #ab28364), anti-nestin (Abcam, #ab6142) or anti-leptin receptor (Abbiotec, #250739), followed by anti-rabbit IgG conjugated to Alexa Fluor 488 (Life Technologies, #A11034) or anti-mouse IgG conjugated to Alexa Fluor 488 (Life Technologies, #A21202).

Flow cytometry. To evaluate the distribution of the various hematopoietic cell populations, flow cytometric analysis was performed using a five-laser Fortessa flow cytometer (Becton Dickinson). Cell types were evaluated on the basis of expression of surface antigens that are characteristic for HSCs, long-term HSCs, hematopoietic progenitor cells and multiple differentiated blood cell lineages. The differential distribution was evaluated according to percentage of whole bone marrow. Because the HSCs and hematopoietic progenitor cell populations represent a small percentage of the total, representative flow cytometry plots are shown after excluding mature lineage-restricted (Lin) cells. The numbers shown on the FACS plots indicate the percent contribution relative to the whole–bone marrow population. For harvesting of bone marrow cells, the eBM was removed from the PDMS devices, cut into small pieces and digested using 1 mg/mL collagenase (Roche) for 30 min. Bone marrow cells harvested from eBM and normal mouse femur were stained in cold PBS containing 3% FBS and 0.05% sodium azide for 30 min with antibodies directed against (i) eFluor 450 hematopoietic lineage cocktail (1:5, eBioscience, #88-7772-72), APC Sca1 (1:333, eBioscience, #17-5981-82, clone D7), APC-eFluor780 cKit (1:160, eBioscience, #47-1172-82, clone ACK2), FITC CD34 (1:50, eBioscience, #11-0341-82, clone RAM34) or APC CD34 (1:10, eBioscience, #50-0341-82, clone RAM34), and PE CD135 (1:20, eBioscience, 12-1351-82, clone A2F10) to identify HSCs ($Lin^-Sca1^+cKit^+$) and progenitor cells (Lin^-Sca1^+, Lin^-cKit^+, Lin^-CD34^+, Lin^-CD135^+); (ii) lineage cocktail (1:5, eBioscience, #88-7772-72), PE CD150 (1:40, eBioscience, #12-1501-82, clone 9D1) and APC CD48 (1:160, eBioscience, #17-0481-82, clone HM48-1) to identify long-term HSCs ($Lin^-CD150^+CD48^-$); or (iii) APC-eFluor780 Ter119 (1:40, eBioscience, #47-5921-82, clone TER-119), Pacific Blue CD45 (1:200, eBioscience, #48-0451-82, clone 30-F11), APC-Cy7 CD3 (1:20, BD Pharmingen, #560590, clone 17A2), APC CD19 (1:80, BD Pharmingen, #550991, clone 1D2), APC-Cy7 Mac1 (1:160, eBioscience, #47-0112-82, clone M1/70) and APC Gr1 (1:160, eBioscience, #17-5931-82, clone RB6-8C5) to identify erythrocytes (Ter119), leukocytes (CD45), B cells (CD19), T cells (CD3) and myeloid cells (Mac1 and Gr1). Cellular viability was evaluated using propidium iodide (25 ng/mL, Millipore).

***In vitro* microfluidic culture on-chip.** The cylindrical eBM was removed from the PDMS device, pierced multiple (4–6) times with a surgical needle (32 gauge) and cultured in a similarly shaped central chamber within a microfluidic chip device (**Fig. 1a**,**b**) that was separated from overlying and underlying microfluidic channels (200 μm high) by porous PDMS membranes (20-μm thick with 100-μm pores). The microfluidic channels were molded against master molds made by standard photolithography using the negative photoresist SU-8 (MicroChem). PDMS membranes were made by spin-coating a PDMS layer on a silanized glass slide (50 mm × 75 mm) at 1,500 r.p.m. for 60 s and then curing in an 80 °C oven for at least 2 h. An array of 100-μm pores with a 100-μm pitch was made on a PDMS membrane using a laser cutter (Versal Laser VL-300, Universal Laser Systems). Microfluidic channel layers and porous PDMS membranes were

doi:10.1038/nmeth.2938

bonded together using a plasma etcher in air for 30 s. To allow introduction of solution into the channels, we punched access holes through the top channel layer with a 2-mm biopsy punch, and the inlets and the outlets were connected with tubes (i.d. = 1/32 inch). The microfluidic device was oxidized using a plasma etcher in air for 10 min to make the PDMS surface hydrophilic. The eBM was inserted into the central chamber (which was bonded to the bottom channel layer) before attachment of the top channel layer. The microfluidic device was placed between two acrylic plates (30 mm in diameter) made by a laser cutter and immobilized using screws (**Fig. 1b**). To maintain cellular viability of the eBM, we perfused culture medium (SFEM basal medium, StemCell Technologies) containing cytokines[32,33] (50 ng/mL mouse SCF, 100 ng/mL mouse IL-11, 100 ng/mL mouse FLt-3, and 20 μg/mL human LDL, StemCell Technologies) through the top and bottom channels (1 μL/min, 0.005 dyn/cm^2) using a syringe pump (BS-8000, Braintree Scientific).

Stroma-supported bone marrow cell culture. Bone marrow stromal cells were harvested from 8- to 12-week-old C57BL/6 mice, resuspended in DMEM medium (Gibco) containing 20% FBS (Gibco), GlutaMAX (Gibco) and 100 units/mL penicillin-streptomycin (Gibco), and were cultured in the same medium on tissue culture plates (Falcon), with the medium changed every other day to create stromal feeder layers. After the adherent monolayer became established (about 3 weeks), the cells were irradiated with 12 Gy. Bone marrow cells harvested from femurs of C57BL/6-Tg(UBC-GFP)30Scha/J mice were cultured on this bone marrow stromal cell layer using the same culture medium used in the microfluidic culture.

Bone marrow transplantation. Bone marrow transplantation was performed on 8-week-old C57BL/6 mice exposed to two doses of radiation measuring 6 Gy separated by 2–3 h. Because these mice were purchased from a vendor and randomized upon arrival, a randomization procedure was not conducted. The bone marrow cells were harvested from femurs of C57BL/6-Tg(UBC-GFP)30Scha/J mice or from eBM produced in similar GFP-labeled mice after 4 d of microfluidic culture. 2.5×10^5 bone marrow cells were delivered by intravenous (i.v.) tail-vein injection within 12 h of lethal irradiation. Engraftment was measured 6 weeks and 16 weeks after transplant using retro-orbital bleeds and flow cytometric analyses.

Micro-computed tomographic (micro-CT) analysis. eBM harvested from mice 4 and 8 weeks after device implantation were fixed for 48 h in 4% paraformaldehyde and stored in 70% ethanol at 4 °C. Vertebrae harvested from the same mice immediately after device removal were handled similarly. Both the eBM and vertebrae were imaged (in 70% ethanol) with an XRA-002 X-Tek MicroCT system. X-ray transmission images were acquired at 55 kV and 200 μA, and the 3D reconstructions were performed using CT-Pro (Nikon Metrology); surface renderings were generated using VGStudio Max.

Compositional backscattered scanning electron (BSE) micrographs and elemental mapping. eBM and vertebrae harvested and fixed as described for micro-CT were serially dehydrated into 100% ethanol and then embedded in Spurr's resin and sectioned at the desired imaging plane using a slow-speed diamond saw. The resulting sections were polished with silicon carbide papers down to P1200, sputter coated with gold and examined using a Tescan Vega-3 scanning electron microscope equipped with a Bruker X-Flash 530 energy-dispersive spectrometer (EDS). All EDS spectra and elemental maps were acquired at 20-keV accelerator voltage. For calculating elemental composition of both the sectioned implant and vertebra samples, ten point spectra from the surface of each sample were acquired, and the percent phosphorous and calcium content was determined by averaging the obtained values ± s.e.m.

γ-radiation. Freshly harvested eBM made in C57BL/6-Tg(UBC-GFP)30Scha/J (Jackson Laboratories) mice, 1×10^7 mouse femur bone marrow cells maintained in stroma-supported culture and 8-week-old C57BL/6-Tg(UBC-GFP)30Scha/J were exposed to one dose of γ-irradiation (Cs-137) at 1 Gy or 4 Gy. 96 h after irradiation, marrow from the eBM cultured on-chip, bone marrow in stroma-supported culture and bone marrow from the femurs of live mice were collected for flow cytometric analysis. 500 U/mL granulocyte colony–stimulating factor (G-CSF, Sigma-Aldrich) was added in the culture medium containing cytokines 24 h after exposure to γ-irradiation. After 72 h in culture on-chip with G-CSF, marrow from the eBM was collected for flow cytometric analysis.

Statistics. Sample size for *in vitro* and *in vivo* experiments was determined on the basis of a minimum of $n = 3$ biological replicates. Statistical differences were analyzed by Student's t-test. All statistical evaluation was conducted using a two-tailed t-test, assuming independent samples of normal distribution with equal variance. $P < 0.05$ was deemed statistically significant; all error bars indicate s.e.m.